

## NUMERICAL INVESTIGATIONS INTO THE CRUSHING BEHAVIOUR OF CONICAL SHELL SYSTEM

A. S. Mokhtar, H. S. Sultan, M.K.Abdullah, E. Mahdi, A.R. Abu Talib and A. M. S. Hamouda  
Faculty of Engineering, Universiti Putra Malaysia, 43400 UPM, Serdang, Selangor, Malaysia  
Email: samsuri@eng.upm.edu.my

### ABSTRACT

*In this paper numerical investigations into the crushing of woven roving laminated conical system have been conducted. Energy absorption capability can be achieved if the longitudinal properties of composite structures are being utilized. This can only be done if the energy absorbing system post failure scenario would be mitigated to be tearing failure mechanism. The system was designed by slipping a solid cone into composite cone. The semi cone angles used were 4, 8, 12, 16 and 20 degrees. The cone height and bottom diameter were kept constant for all cases as 100 mm and 76.2 mm, respectively. The results demonstrated that at first crush stage the energy is dissipated in the form of friction and the conical responded in an elastic manner, while the post crush stage is dominated by tearing failure mechanisms.*

**Keywords:** optimization; tearing mechanisms. composite; energy absorber; cone

### INTRODUCTION

Lightweight energy-absorption structures in airframes or aerospace structure and automotive vehicles are increasingly used to meet the crashworthiness requirements with a minimum weight increase. Since the last two decades, composite materials are used extensively to build aircraft structure. However, those crashworthiness criteria related to composite structures has becomes an important issue for many space organizations worldwide. For example, NASA Langley Research Centre developed some innovative and cost effective crashworthy fuselage concept for light aircraft and rotorcraft. In other research related work, a new composite energy absorbing system for aircraft and helicopter has been developed by the author and other co-researcher [1]. Hence, this work is also an extension of the extensive work to understand the crashworthiness behaviour of composite and effect of its configurations.

Crashworthiness may be defined as the ability of a vehicle to protect its occupants from death or serious injury in an accident of a given severity. Simply, the ability of a restraint system or component to withstand loads below a certain level and to reduce the damage caused in those cases involving excessive dynamic loads [2]. In high performances automotive, these absorbers are used to improve the vehicle safety in case of frontal, rear or lateral impacts. These devices placed between the frame and the chassis, it can reduce the acceleration peaks transmitted to the occupancies. In aerospace field, energy absorbers are used in helicopter sub-floors or in light aircrafts to reduce the consequences of an impact with the soil in emergency landing or after an accident [3].

It is well understood that composite structures exhibit distinct failure mechanisms in crushing that are dependent upon the material properties, geometry and the loading condition [3-5]. Because wide-ranging of loading conditions are possible in a crushable energy absorber devices during an impact event, it is important to understand the behaviour of these devices under different loadings, including pushing in loading conditions. However, there is a paucity of experimental and finite element work on the quasi-static as well as dynamic pushing of solid structures into hollow composite thin walled shell structure. The use of composite in designing energy absorption system requires an insight into the failure modes that are unique to these types of materials. Unlike fractures, highly crazed surfaces can transmit energy. Crazes are the first sign of surface tensile failures in thermoplastic materials and gel coat finishes. Crazes appear as clean hairline fractures extending from the

surface into the composite. Crazes are not true fractures, but instead are combinations of highly oriented “fibrils” surrounded by voids. Depending on the application, any tear in a material may be considered a failure or some tearing may be allowed, provided the structure can absorb the required energy or carry the specified load. In both cases, a strain-to-failure value is generally used as the tearing criterion. The developed system can also be used in the packaging system of heavy and light goods [6-7].

## CRASHWORTHINESS PARAMETERS

### Crush Force Efficiency (CFE)

The wide exploitation of advanced composites in energy absorber designs will depend to a large degree on the ability to support loads (average crush loads) well beyond the initial failure stage, which minimize second impact. This could be well demonstrated by evaluating the crush force efficiency (CFE), which can be calculated as

$$CFE = \frac{P_m}{P_{pH}} \quad (1)$$

Where,  $P_p$  and  $P_m$  represent peak and mean crush load, respectively. The later can be obtained by averaging the crush load values over the crush displacement though the post-crush stage, while the former can be directly obtained from the load-displacement curve as the peak load value at initial failure stage. For optimum crush unit, the CFE should be equal to one [8].

### Energy absorption Capability

Two types of energy absorption, during slipping solid con into conical shells were measured. These are the energy absorbed per unit mass ( $E_s$ ) and energy absorbed per unit volume ( $E_v$ ). The former represents total work done ( $W_T$ ), which is equal to the area under the force-stroke curve [9-10]

$$W_T = \int_{s_p}^s P_i ds \quad (2)$$

The post-crush stage is generally more important due to its strong influence on the crashworthiness parameters. Therefore, work done at post crush stage ( $W_p$ ) can be calculated as:

$$W_p = \int_{s_p}^s P_i ds \Rightarrow P_m (S - S_p) \quad (3)$$

Energy absorbed per unit mass (i.e. specific energy absorption)

$$E_s = \frac{W_p}{M} \quad (4)$$

By substituting Equation 5 into 4

$$E_s = \frac{P_m (S - S_p)}{\rho \times V_i} \quad (5)$$

For complete crushing i.e.  $s=L$ , Eq. 6 can be re-written as

$$E_s = \frac{P_m (S - S_p)}{\rho \times V} = \frac{P_m \left( \frac{S}{L} - \frac{S_p}{L} \right)}{\rho \times A} = \frac{P_m (1 - SE_p)}{\rho \times A} \quad (6)$$

As stated earlier, the specific energy is not the only crucial design factor for energy absorber device crashworthiness performance; the energy absorbed per unit volume is also essential, where the space is a restraint. The volume occupied by the WRL conical shells before crushing (i.e. at preloading state) can be calculated as

$$V_{con} = \frac{\pi H}{12} [D^2 + Dd + d^2] \quad (7)$$

The energy absorbed per unit volume  $E_v$  can be calculated as

$$E_v = \frac{P_m (S - S_p)}{V_{con}} \quad (8)$$

## FINITE ELEMENT ANALYSIS

Numerical simulation was carried out. The finite element simulation was designed to predict the load-displacement curves, deformation histories and energy absorption capability throughout the E-glass fibre fabricated and semi- cone angles.

### Model Development

LUSAS finite element package was performed the numerical simulation for the quasi-static method. Detailed three-dimensional finite element modes of glass fibre fabricated and semi-vertex angle conical curved composite systems were developed. Composites are somewhat more difficult to model than an isotropic material such as iron or steel. We need to take special care in defining the properties and orientations of the various layers since each layer may have different material properties. In this section will be described finite element techniques that used in this study. A complete finite element analysis involves three stages: Pre-Processing, finite element solver and results-processing. Finite element system consists of two parts to perform a full analysis:

- Modeller is a fully interactive pre- and post-processing graphical user interface.
- Solver performs the finite element analysis.

Typical meshes generated, was in Fig.1 consist of 6291 nodes, 3168 elements, 5775 nodes, 3168 elements, 5648 nodes, 2624 elements and 5480 nodes, 1960 elements for the semi vertex angles 4, 8, 12, 16, and 20 respectively.

Three-dimensional continuum element (HX20), twenty-nodes quadratic interpolation order with hexahedral element shape, (HX20) element was used since this is expected to give accurate stress and strain results. This type of element was chosen for modelling these systems for static non-linear analysis prediction. Each node has six degrees of freedom, which include three displacements,  $u_x$ ,  $u_y$ ,  $u_z$ , and three rotation components,  $\theta_x$ ,  $\theta_y$ ,  $\theta_z$ . This element is expected to be more accurate compared with others elements. The laminate was modelled by defining each lamina with material properties, thickness and fibre orientation. Fully fixing degrees of freedom at one end of the model and applying the load at the other end by using a prescribed displacement simulated the testing conditions. Numerical simulation for the specimens is run until complete failure crush load is reached.

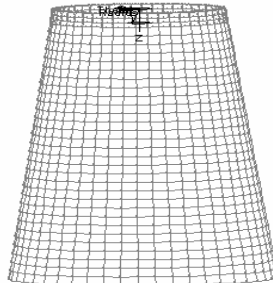


Fig.1: Typical Mesh Generation of WRL Conical Shell

## Material Properties

This section refers to material types used to model; orthotropic material properties were used from the library of the LUSAS code in development of finite element analysis [11]. The basic material properties required for this model are orthotropic elastic properties given in Table 1, and orthotropic damage properties by using Oliver's model as its shown later.

Table 1. Material Properties of glass fibre/Epoxy

Material Property	Symbol	Property Value
Young's Modulus in x-direction	$E_x$	20 GPa
Young's Modulus in y-direction	$E_y$	19 GPa
Young's Modulus in z-direction	$E_z$	8 GPa
Shear modulus in xy-direction	$G_{xy}$	4.2 GPa
Shear modulus in xy-direction	$G_{yz}$	4.2 Gpa
Shear modulus in xy-direction	$G_{xz}$	4.2 Gpa
Poison's Ratio	$\nu_{12}$	0.13
Mass density	M	1900 kg/m <sup>3</sup>

## Damage Models

Damage is assumed to occur in a material by the initiation and growth of cavities and micro-cracks. The damage properties data chapter allows parameters to be defined which control the initiation of damage and post damage behaviour. In finite element analysis a scalar damage variable is used in the degradation of the elastic modulus matrix. This means that the effect of damage is considered to be non-directional or isotropic. To model an isotropic damage process it suffices to consider a scalar damage variable  $d$ . The damage models under a type of stress-based elastic-damage model, in which the damage is determined by a norm of elastic complementary energy [11].

### Oliver's Damage Model

The damage criterion for the Oliver model introduces a factor which is involved if different stress levels cause initial damage in tension and compression. The initial damage threshold,  $r_o$ , can be considered to carry out a similar function to the initial yield stress in an analysis involving an elastic-plastic material. However, in a damage analysis, the value of the damage threshold influences the degradation of the elastic modulus matrix. A value for the initial damage threshold ( $r_o$ ) may be obtained from:

$$r_o = \frac{\sigma_t}{E^{0.5}} \quad (9)$$

Where  $\sigma_t$  is the uniaxial tensile stress at which damage commences and  $E$  is the undamaged Young's modulus. The damage accumulation functions for each model are given by:

$$G(r) = 1 - \frac{r_o}{r_t} \text{Exp}[\lambda(1 - \frac{r_o}{r_t})] \quad (10)$$

For no damage,  $G(r) = 0$ , the characteristic material parameter,  $\lambda$  would generally be obtained from experimental data. However, a means of computing material parameter ( $\lambda$ ) has been postulated for the Oliver model:

$$\lambda = \left[ \frac{G_f E}{L_{ch} \sigma_t^2} - \frac{1}{2} \right]^{-1} \quad (11)$$

Where  $G_f$  is the fracture energy per unit area,  $L_{ch}$  is a characteristic length of the finite element which can be approximated by the square root of the element area, ( $L_{ch}$  from 0.05 to 0.15). The Damage ratio is the ratio of the tensile stress to compressive stress that causes initial damage in tension and compression [10].

$$D_r = \frac{\sigma_c}{\sigma_t} \quad (12)$$

## RESULTS AND DISCUSSION

The load-deformation curves with failure mechanisms give out an indication to determine how and when forces and moments change throughout the structures. This can then be used to determine the energy, which is an important input for the design of vehicle structures. Load-displacement curves were obtained from LUSAS finite element. A comparison of load-displacement curves have been made to initial crushing load, highest crushing load, mean crushing load and load carrying capacity for all the models of semi-vertex angles of 4, 8, 12, 16, and 20 degrees. The load-displacement relations of these structures are collected and shown in Figure 3. From these relations, the results included the initial failure load for each specimen, the mean crushing load, highest crushing load (maximum crushing load) and crush energy absorption that represented the area under the curve.

### Effect of cone vertex angle

Figure 3 shows the force-displacement response of conical shells to solid steel cone slip axially. From the figures, it can be noticed that the conical shell with semi cone angle of 8 degrees has the highest resistance. The crushing force at pre-initial crush stage increases almost linearly until its first peak value of 8.2kN at 0.13 mm displacement. Matrix failure mechanism of micro cracking initiated at the top end of the cone, this led the load-displacement curve to small dropped from 8.2kN to 7.1kN at 0.35mm displacement (mm) this occurs because of matrix cracking and tearing failure mode in most inner cone wall layer at small end of cone. Then the load rises and reaches to 9.2kN at 2.17mm. Then, load-displacement curve behaviour becomes almost stable and it's fluctuating about 9.5kN from 2.17mm displacement to the end of crushing during the post crush stage. The mean crush load ( $P_m$ ) value was 9.2kN. However, in pre-initial crush stage no damage is visible through the finite element analysis and the elastic energy absorbed by conical shell. While in post crush stage, the energy absorbing mechanisms were found to be significantly depending on the specimen scenario failure modes.

### Initial Failure Load ( $P_i$ )

The initial failure load is defined as the first point where the load abruptly decreases after the elastic linear increase of load. The initial failure load for each test has been obtained directly from the load-displacement curve as shown in Fig. 3. From the curve obtained Fig. 4, it appears that the initial failure load was decreasing with the increase of semi-vertex angle of cone. These results are also listed in Table 2.

### Mean Crushing Load ( $P_m$ )

The mean crushing load is the average crush load can be obtained by averaging the crush loads values over the crush displacements through the post-crush region. It is appears from Fig. 5 that the mean crushing load also decreases as the semi-vertex angle of cone increases.

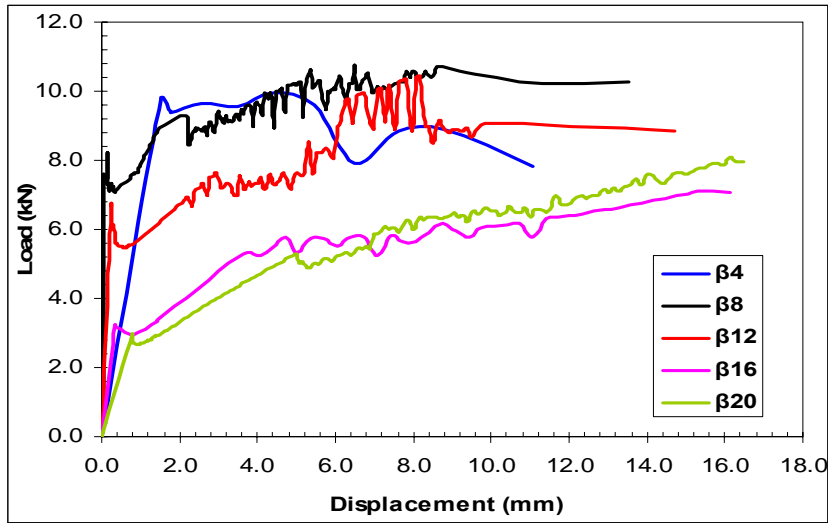


Figure.3: Finite element load-displacement curves of WRL semi cone angles system under slipping crush test

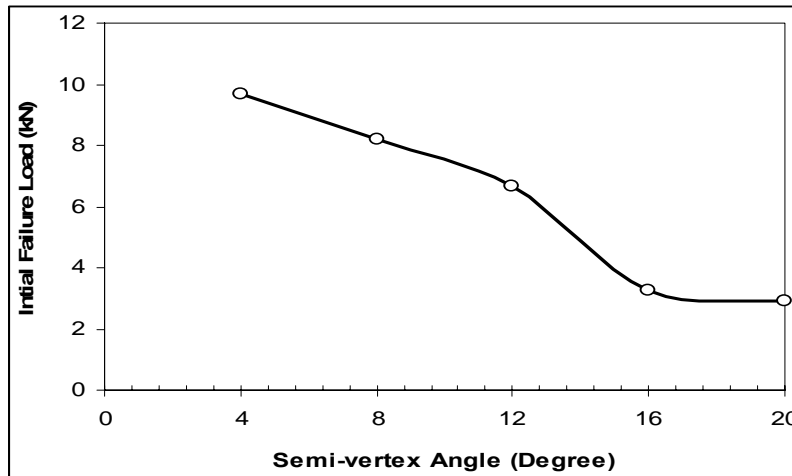


Figure 4: Initial failure load Vs semi-vertex angles of conical shells

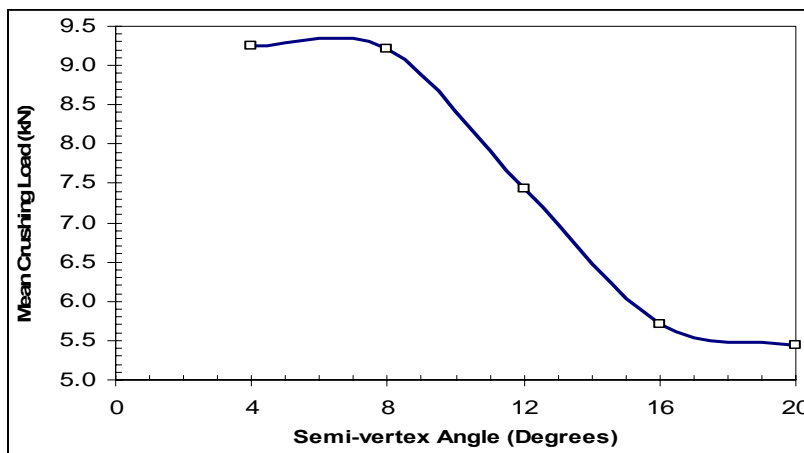


Figure 5: Mean crushing load Vs semi-vertex angles of conical shells

Table 2: Measured crashworthiness parameters for the slipping of solid steel cone into the woven roving wound laminated glasslepo xy conical shells

Cone ( ID)	P <sub>i</sub>	P <sub>m</sub>	P <sub>pH</sub>	IFI	CFE	SE	E <sub>s</sub>	E <sub>v</sub>
	(kN)			kN/kN		mm/mm	kJ/kg	(kJ/m <sup>3</sup> )
β4°	9.70	9.26	9.9	0.85	0.91	0.74	0.76	202.75
β8°	8.21	9.22	9.9	0.83	0.94	0.76	1.29	417.1
β 12°	6.69	7.43	10.2	0.66	0.72	0.65	1.20	484.75
β 16°	3.25	5.71	7.0	0.45	0.80	0.66	0.99	493.6
β 20°	2.92	5.44	8.2	0.35	0.67	0.52	0.97	608.9

### Energy Absorption Capability

The energy absorption represents the area under the load-displacement curve for each one. As stated earlier and from Equations 4, 5 and 9, there are two types of energy absorption, during slipping solid cone into conical shells were measured. These are the energy absorbed per unit mass (E<sub>s</sub>) and energy absorbed per unit volume (E<sub>v</sub>). Figure 6 represented the relations between specific energy absorption and volumetric energy absorption as a function of semi-vertex angles of composite conical shell. It is interested to note that the model with semi-vertex angle β of 8 degrees exhibited more resistance to slipping the solid steel cone through the crush that's means more stable deformation as well as structural integrity. This resulting in higher energy absorption compared with other models. One of more important observation is that most of energy absorption process occurred in post-crush stage as clearly shown from Figure 3 that the post-crush stage for semi-vertex angle β of 8 degrees was more stable than that for β of 4, 12, 16 and 20 degrees and during this stage, The specific energy absorbed by the cone with semi-vertex angle β of 8 degrees was 1.29 kJ/kg. These results for crush energy absorption were also tabulated for all the tests in Table 2. From Table 2 the specific energy absorption of β8° was quite high compared with others cones. As mention earlier the volumetric energy absorption capability (E<sub>v</sub>) was calculated used Equation 9 The presence of the resistance mechanism in β8° increases their crashworthiness parameters. From the energy absorption capabilities and crashworthiness parameters points of view one can deduced that the composite conical shells with semi-vertex angle β of 8 degrees have superior energy absorption compared to the other cones.

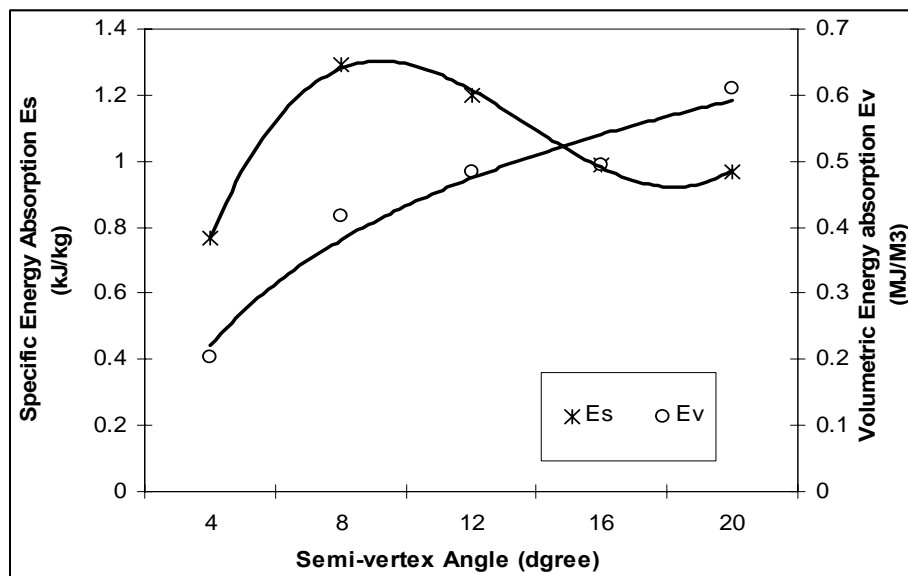


Figure 6: Energy Absorption Capabilities as Function of Semi-vertex Angles of Composite Conical Shells

### Failure Modes

As the slipping of the solid steel cone continues, a pattern of damage distinctive to thin walled conical shells axially crushed between two platens begins to appear. In Fig. 7, the accumulation of local damage at the contact between the solid cone and the conical shell wall is evident. With continued slipping of the solid cone and growth of damage, the innermost layer experiences compression state. This resulted in that the outer most layers materials properties degraded quickly, and the innermost layer begins to tear away. The tearing failure mode is longitudinal fibres and occurs near the contact area between the solid steel cone and the conical shell wall. Subsequently, the tearing failure becomes the predominant mode of damage, and proceeds down the along the shell generator as the solid steel cone travel increases.

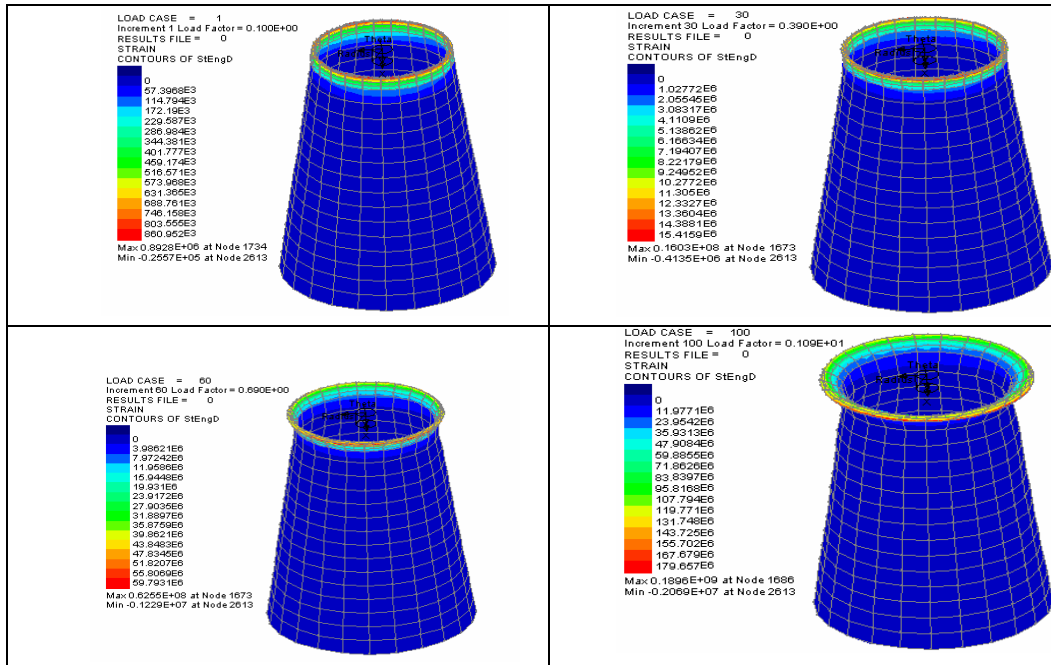
### CONCLUSION

An out-of-plane tearing damage mode has been experimentally identified. This behaviour is beneficial in that the structure is capable of absorbing impact energy in the form of material separation. Conical shells crushed by slipping solid cones have been shown capable of absorbing considerable energy in uniform load-displacement behaviour. Sudden large drops in load are related to the vertex angle. The magnitude of the load drops depends on the failure mode failure mechanism.

Specimens crushed in a progressive manner show limit high-impact loads. It is seen that the entire failure mechanism is initiated by matrix cracks, which result in delamination at layers interfaces. The energy absorption capability of semi cone angle  $\beta=8^\circ$  subjected to slipping test was greater than the energy absorption of semi cone angles 12, 16 and 20.

### ACKNOWLEDGEMENTS

The authors wish to thank Universiti Putra Malaysia for the financial support for this research programme.





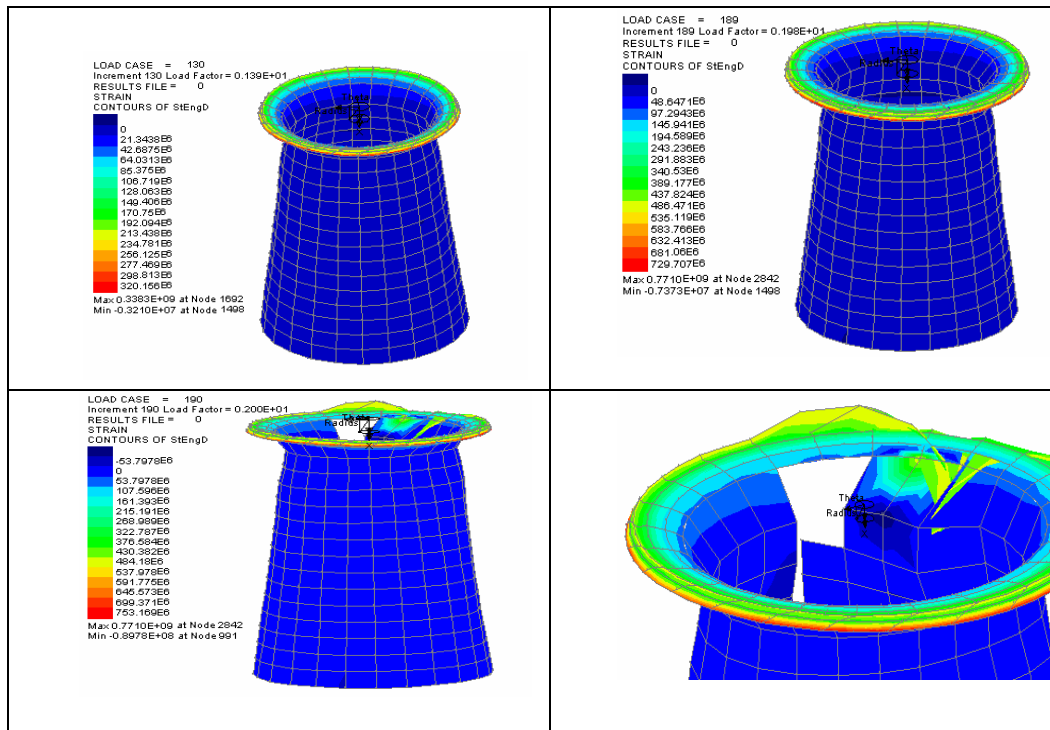


Figure 7: Deformed shape of semi cone angle with  $\beta = 8^\circ$  subjected to the slipping system

## REFERENCES

- [1] S.T.Taher, E.mahdi, A.S.Mokhtar, D.L.Magid, F.R.Ahmadun and P.R.Arora (2006). A new composite energy absorbing system for aircraft and helicopter, *Composite Structures*, **75**: 14-23.
- [2] Farley, G. L. and R. M. Jones. 1989. Energy-Absorption Capability of Composite Tubes and Beams, NASA TM 101634.
- [3] Farley, G. L. (1983). Energy Absorption of Composite Materials, *Journal of Composite Materials*, **17**(5): 267-279.
- [4] Hull, D. (1991). A Unified Approach to Progressive Crushing of Fibre-Reinforced Composite Tubes, *Composites Science and Technology*, **40**: 377-421.
- [5] Farley, G. L. and R. M. Jones. (1992). Crushing Characteristics of Continuous Fibre-Reinforced Composite Tubes, *Journal of Composite Materials*, **26**(1): 37-50.
- [6] Fleming, D. C. and A. J. Vizzini. (1992). The Effect of Side Loads on the Energy Absorption of Composite Structures, *Journal of Composite Materials*, **26**(4): 486-499.
- [7] Fleming, D. C. and A. J. Vizzini. (1993). Tapered Geometries for Improved Crashworthiness under Side Loads, *Journal of the American Helicopter Society*, **38**(1): 38-44.
- [8] E.Mahdi, A.M.Hamouda and B. B Sahari. (2002). Axial and lateral crushing of the filament wound laminated composite curved compound system: *Journal of adv.comp. Mater.* **1**: 171-192
- [9] Fleming, D. C. (1991). The Energy Absorption of Graphite/Epoxy Truncated Cones, Master's Thesis, University of Maryland
- [10] Sen, J. K. and C. C. Dremann. (1985). Design Development Tests for Composite Crashworthy Helicopter Fuselage, SAMPE Q
- [11] LUSAS/standard User's Manual, LUSAS theory manual, version 13.5.